Int J Adv Manuf Technol
DOI 10.1007/s00170-016-9187-y

ORIGINAL ARTICLE

# Analysis of flow field for electrochemical machining metal screw pump stator

**Feng Yang[1] · Tianyi Ren[1] · Hongbo Wang[1] · Bingxin Liu[1] · Ming Chen[1]**

Received: 2 March 2016 / Accepted: 13 July 2016
© Springer-Verlag London 2016

**Abstract** The electrochemical machining (ECM) is used to solve the difficult machining problem of metal screw pump stator inner hole; the mathematical model of electrolyte flow field in machining gap is established, and the distribution of electrolyte flow field in ECM machining gap of processing screw pump stator inner hole is simulated by using COMSOL simulation software. The simulation results show that, at the end of the machining gap, the electrolyte is not full, therefore setting up the added liquid hole on the cathode working zone by optimizing the cathode structure in the relevant machining gap zone to improve the distribution of flow field. Finally, the experiments are carried out which were conducted with different voltage and feed rate parameters; the test piece is sliced and measure it after the experiments, based on the measurement results to adjust the process parameters. The experiments result show that, when the processing voltage is 16 V and the feed rate is 6 mm/min, the distribution of electrolyte flow field in machining gap is more uniform, and the test piece size reached the product requirements. The simulation greatly shorten the cathode design cycle and optimize the structure of cathode by using COMSOL.

**Keywords** Screw pump · Electrochemical machining (ECM) · Machining gap · Flow field

✉ Feng Yang
yfwfy0817@163.com

[1] Qigihaer North Machinery Co. Ltd., Qiqihar, Heilongjiang, China

## 1 Introduction

Electrochemical machining (ECM) is using the principle of metal electrochemical anodic dissolution in the electrolyte, that is a method of machining which takes the workpiece as anode, tool as cathode, low voltage and high current density of DC, or pulse current between them; the high pressure of electrolyte pass through the two poles, and the workpiece is dissolved under the effect of electric field; finally, the product with a certain size precision is obtained. ECM has become an indispensable method in advanced manufacturing technology; it can easily machine the difficult machining material, molding for complex shape parts, and has good surface quality, high productivity, no tool loss, no cutting stress, and other unique advantages [1]. With the emergence of new technology and new material, the application of ECM has gradually expanded in aerospace, automobile, electronics, mold, and other fields, and it plays an important role in manufacturing.

The screw pump is mainly used in the field of oil exploitation, which belongs to one kind of oil exploitation equipment in oil machinery [2]. The screw pump is a volume delivery pump, which consists of two parts stator and rotor; it is an application of the cycloidal internal meshing helical gear pair. When the rotor and stator relative rotation, the enclosed chamber which formed in space by using the cycloidal movement characteristic was moved along the axial, and the liquid moved with the enclosed chamber from one end to the other and realize the lifting function. Moineau invented the single-screw pump widely used in hydraulic machinery in the mid 1930s, gradually developing for oil exploitation [3]. At present, the screw pump used in the oil industry consists of two parts, namely rubber stator and metal rotor. This kind of screw pump, due to the restriction of rubber stator, cannot be used in the high-temperature wells, high viscosity wells, and high sediment concentration wells, or its service life is very

Published online: 25 July 2016




Full-Metal-Power B.V. EX. 1006

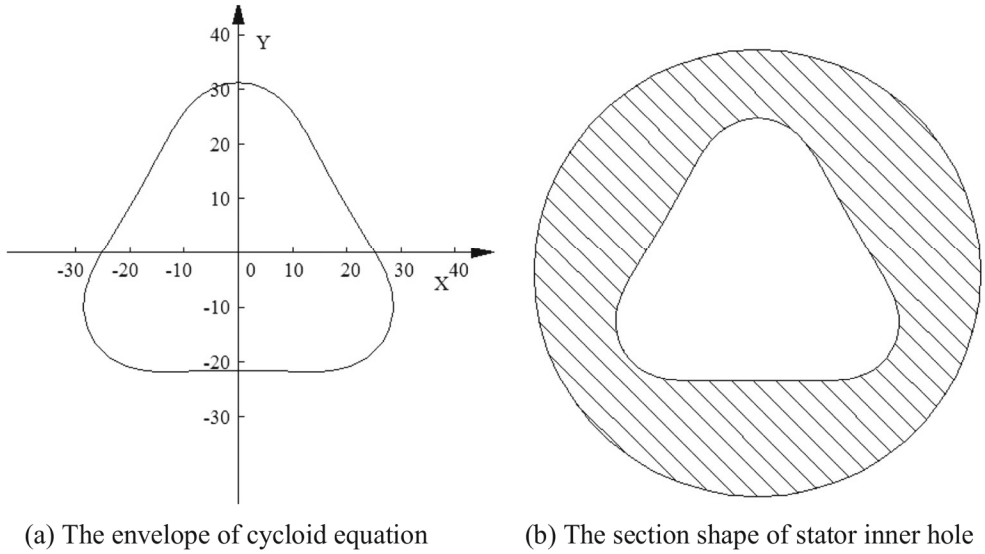


**Fig. 1** The section shape of stator inner hole. **a** The envelope of cycloid equation and **b** the section shape of stator inner hole

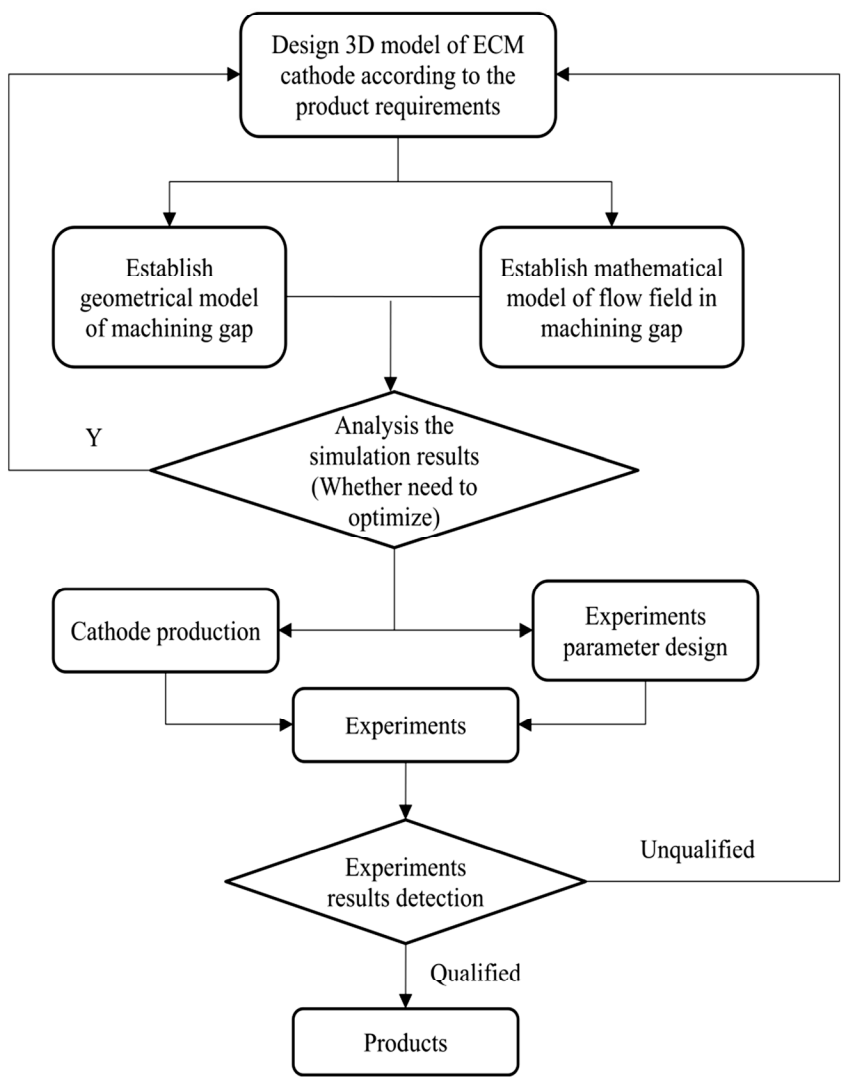


**Fig. 2** Flow chart of ECM processing the metal screw pump stator inner hole

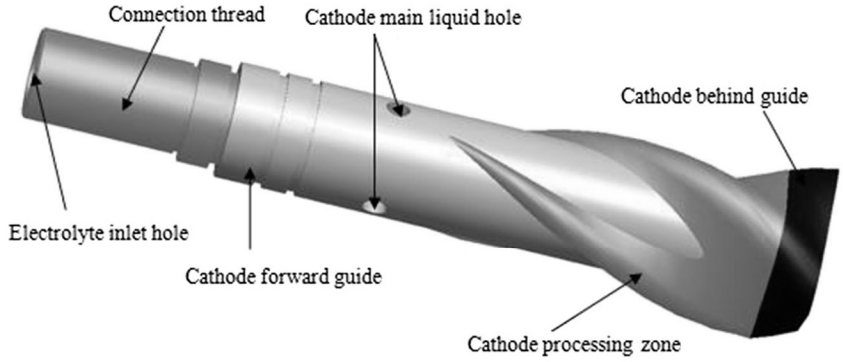


**Fig. 3** The 3D model of cathode in electrochemical machining of screw pump

shorten; also, the cost of replacement and repair of the screw pump in these wells are great. Therefore, the design idea of all-metal screw pump is proposed, which is composed of metal material stator and metal material rotor [4]. Because the all-metal screw pump is used in harsh environment, we put forward higher requirement on the physical and chemical properties of metal stator, which should be corrosion resistance and high temperature resistance; the stator inner surface should also have high hardness and wear resistance due to the rotation between stator and rotor [5]. If the all-metal screw pump is successfully developed, it can replace the rubber screw pump and effectively improve the service life of the screw pump, greatly reducing the costs of replacement and repairment [6].

The difficulty in developing an all-metal screw pump stator is in the metal stator machining, especially the inner hole machining, and there is no feasible method for the machining of the spiral structure of inner hole. The problem of stator inner hole forming is the bottleneck of the all-metal screw pump development [7]. In order to solve the above problem, this paper proposes the ECM method to realize the inner hole forming process of an all-metal screw pump stator, which characteristics are the most suitable for the inner spiral hole forming process.

In this paper, the distribution of electrolyte flow field in ECM machining gap of screw pump stator inner hole processing is simulated by using the COMSOL simulation software. Through analyzing the simulation results of the electrolyte flow field distribution in machining gap to optimize the cathode structure, the development cycle is shortened. The experiments which are conducted with different process parameters are carried out, and according to the measurement results, it optimize the process parameters, and improve the process precision and stability.

## 2 Simulation analysis

In this paper, we take the metal screw pump stator as the research object. We simulate the distribution of electrolyte flow field in machining gap by using COMSOL multiphysics coupling software. We established the mathematical model of flow field in accordance with the flow equation of incompressible fluid; the simulation boundary conditions are based on the ECM process parameters. The comparison of the simulation results and the process experiments analyzes the distribution of flow field in ECM processing gap to optimize the cathode structure and shorten the design and manufacture cycle of cathode.

The envelope of the internal cycloid equation is the section shape of all-metal screw pump stator inner hole, shown in Fig. 1a.

$$\text{Cycloid equation} \quad \begin{aligned} x &= 9.6\cos(t) + 4.8\cos(2t) \\ y &= 9.6\sin(t) - 4.8\sin(2t) \\ & \quad t, \text{ eccentricity } 9.9\,\text{mm} \end{aligned}$$

The envelope of cycloid equation is the section shape of all-metal screw pump stator inner hole, shown in Fig. 1b. And the section shape rotate with a certain lead become the metal screw pump stator inner hole.

The cathode is designed based on the ECM principle and stator inner hole section shape. By using COMSOL software to simulate the electrolyte flow field in ECM processing stator inner hole gap, the distribution law of flow field in processing gap and the influence of ECM on processing all-metal screw pump stator inner hole are researched. According to the simulation results, the cathode structure is optimized. We carry out the ECM processing experiments with different parameters to obtain the test pieces and the measurement results and to verify the accuracy of the simulation results. The flow chart is shown in Fig. 2.

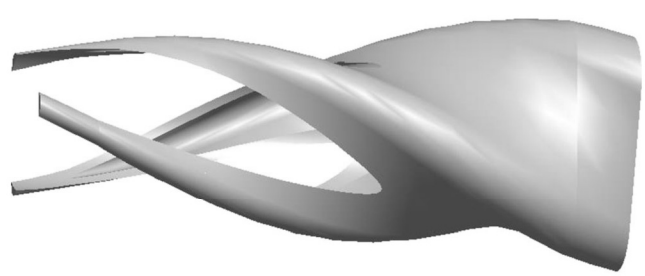

**Fig. 4** The 3D model of electrolyte flow field

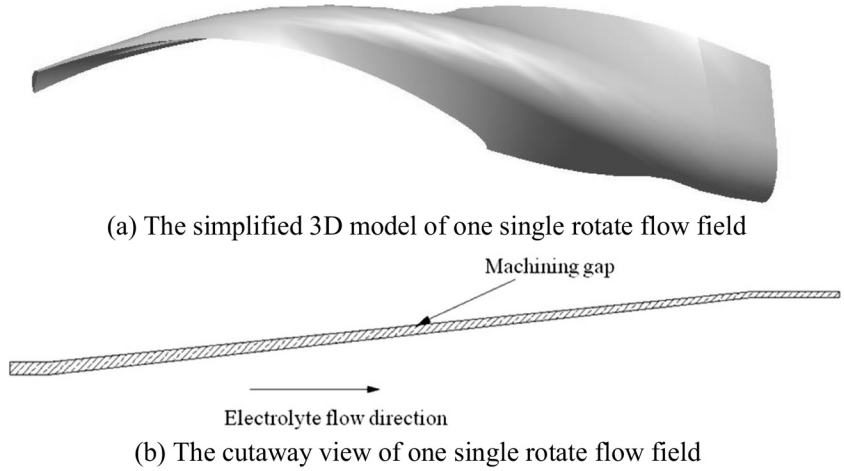


(a) The simplified 3D model of one single rotate flow field

(b) The cutaway view of one single rotate flow field

**Fig. 5** The simplified geometry model of electrolyte flow field. **a** The simplified 3D model of one rotate flow field and **b** the cutaway view of one single rotate flow field

### 2.1 Establishment of geometric model

In ECM process, the cathode is used as a tool, whose research and design are the most complicated work and the key point of ECM [8]. The shape and size of cathode directly determine the size and shape of the product, for different processing object and different molding method, and the design of the cathode is completely different [9].

Cathode design includes the structure design and molding surface (processing surface) design. Structure design refers to a combination of cathode forms and components, and to consider conducting and insulating, clamping and sealing, diversion and flow field, and other issues, the structure design reasonable or not is the primary condition for the stability and efficiency of the products processing under the appropriate parameters [10]. The design of the molding surface (processing surface) is based on the forming rule to design the dimensional and shape of the cathode processing surface [11]. The cathode molding surface is the basic guarantee of the dimensional and shape accuracy of the product.

According to the section shape of screw pump stator inner hole, the cathode model is preliminary designed and established in 3D model by using modeling software. The model is shown in Fig. 3.

The cathode consists of three parts: connection thread, cathode forward and behind guide, and cathode processing zone. The connection thread screw with machine pull rod, so that the machine can drive the cathode to move. The cathode forward guide fitted with the test piece inner hole played a guiding and sealing function, whereas the cathode behind guide played a role in guidance and diversion. The electrochemical reaction occurs at cathode processing zone, which gradually change the width and height from the forward guide to behind guide along to the screw pump stator lead; the final shape is consistent with the shape of the inner hole section of the screw pump stator.

The electrolyte has an outside and inside flow field; the outside flow field is the machining gap and the inside flow field is the electrolyte flow in the cathode. The electrolyte fluid flows through the cathode electrolyte inlet hole and out from the cathode main liquid hole; the electrolyte flows along the cathode processing zone and fill the entire machining gap, then it flows out from the cathode behind guide, finally forming the electrolyte flow field model.

Based on the COMSOL simulation idea of fluid, we put the electrolyte flow field in machining gap as the simulation object [12]. So the 3D geometric model of flow field in processing gap is established as the research object, the area of the electrolyte flow is an entity, and the area without electrolyte is empty, whereas the geometrical model is taken as the carrying medium of the fluid parameters. The 3D geometry model of electrolyte flow field in the gap is shown in Fig. 4.

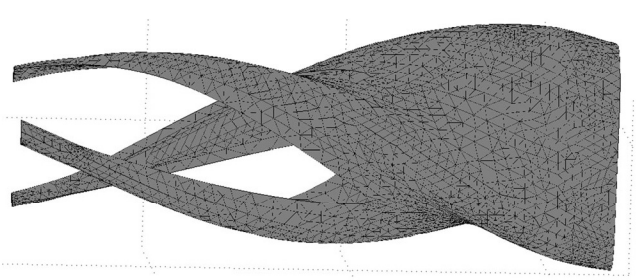

**Fig. 6** Electrolyte flow field meshing in processing gap

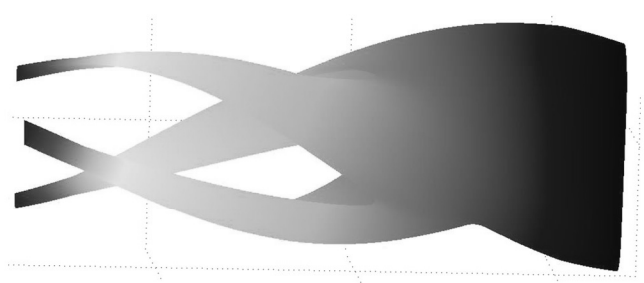

**Fig. 7** Simulation result of electrolyte flow field in machining gap

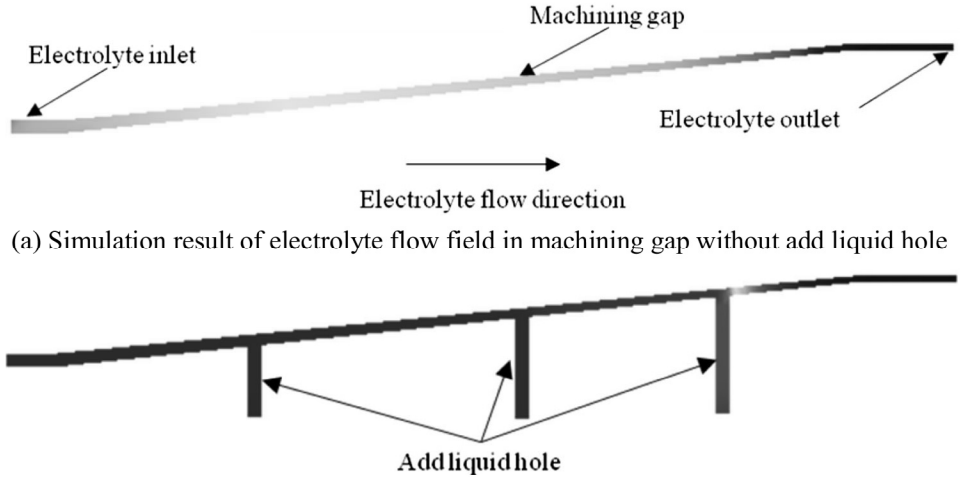


(a) Simulation result of electrolyte flow field in machining gap without add liquid hole

(b) Simulation result of electrolyte flow field in machining gap after set up add liquid hole

**Fig. 8** Cutaway view of simulation results of electrolyte flow field in machining gap. **a** Simulation result of electrolyte flow field in machining gap without add liquid hole and **b** simulation result of electrolyte flow field in machining gap after set up add liquid hole

In order to directly analyze the distribution of the flow field in the machining gap, the geometry model is simplified, as shown in Fig. 5a. According to the 3D model of electrolyte flow field, the flow field can be divided into the same three parts that rotate along the axis and distribute uniformly. In the simulation analysis, one single rotate flow field can indicate the whole flow field. As shown in Fig. 5b, we make the cutaway view of one single rotate flow field, the simplified geometric model of electrolyte flow field as shown in Fig. 5.

### 2.2 Establishment of mathematical model

The hypotheses of flow field mathematical model in ECM processing gap are as follows: (1) the fluid is an incompressible constant Newton fluid, which is the dynamic viscosity constant when velocity gradient changed; and (2) the electrolyte flow field in processing gap is a turbulent state, neglecting the change of electrolyte concentration and temperature during the processing and the loss of energy caused by the change [13–15]. The flow of the electrolyte is constrained by the law of mass conservation and momentum conservation.

The motion equations of incompressible fluid flow in fluid mechanics are Navier Stokes equations. The electrolyte flow in ECM processing gap should be satisfied.

$$\rho u \cdot \nabla u = \nabla\left[-pI + \eta\left(\nabla u + (\nabla u)^T\right)\right] + F \tag{1}$$

$u$ is the electrolyte flow rate (m/s), $\rho$ is the electrolyte density (kg/m$^3$), $\eta$ is the dynamic viscosity (Pa s), and $F$ is the volume force (N/m$^3$).

The volume force ($F$) of electrolyte caused by the mutual movement of cathode and anode in the processing gap is very small and can be neglected. The electrolyte density $\rho$ is $1.1 \times 10^3$ kg/m$^3$. The dynamic viscosity is $\eta = \frac{P_v}{\nu}$, $\nu$ is the kinematic viscosity coefficient, related to temperature, when electrolyte temperature is 35 °C, and the kinematic viscosity coefficient is $\nu = 0.73 \times 10^{-10}$ m$^3$/s.

The viscous friction pressure of electrolyte in processing gap is as follows:

$$P_\gamma = \lambda \frac{L}{D_h} \times \frac{\rho u_0^2}{2} \tag{2}$$

$L$ is the flow length in gap $L = 0.025$ m, $Dh$ is the hydraulic diameter 0.0015 m, $\lambda = \frac{0.3164}{R_e^{0.25}}$, and $Re$ is Reynolds coefficient. In order to remove the electrolytic product in the anode surface and reduce concentration polarization, the electrolyte flow must be turbulent state.

$Re = \frac{uD_h}{\nu}$, $Re > 2300$ is turbulent state.

The electrolyte flow rate at the entrance of gap is determined by

$$u_0 = \frac{U_R i}{\rho \Delta_0 C \Delta T_e} = \frac{i^2}{\rho \kappa C \Delta T_e} L \tag{3}$$

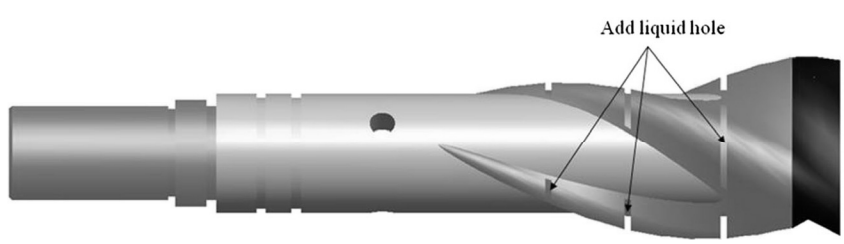


**Fig. 9** The cathode structure after set up add liquid hole

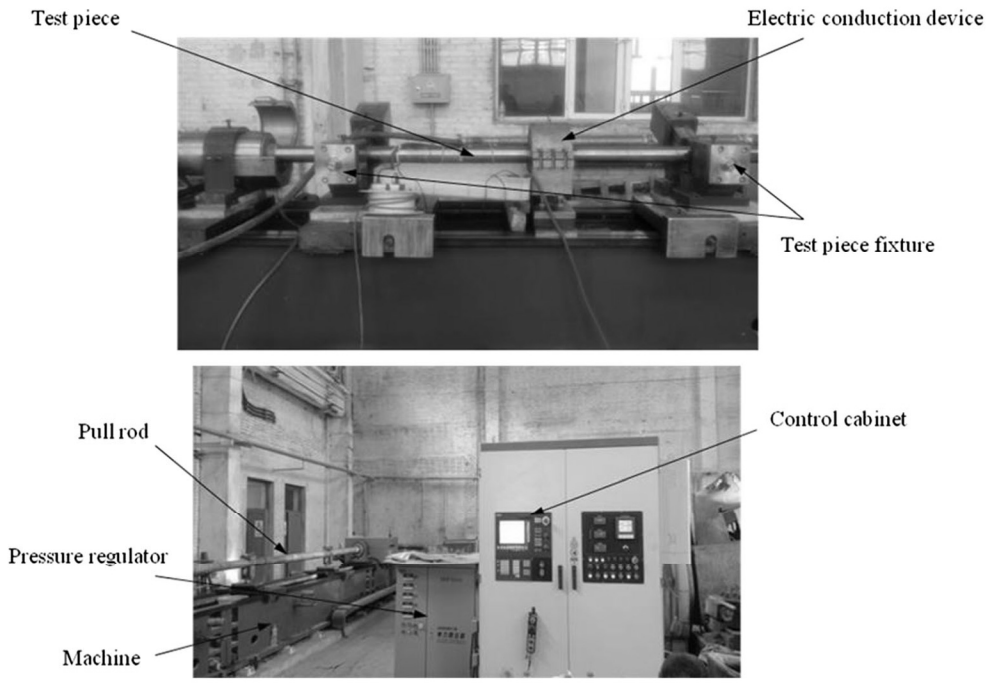


**Fig. 10** DJW-08 CNC horizontal ECM machine

$L$ is the flow length in gap, $T_0$ is the reference temperature, $T_e$ is the temperature after processing, $\Delta T_e$ is the temperature range 5 °C, $i$ is the current density, $\rho$ is the electrolyte density $1.1 \times 10^3$ kg/m$^3$, $\kappa$ is the electrolyte conductivity 17 (1/Ω m), and $C$ is the electrolyte-specific heat $C = 4.03 \times 10^3$ J/kg.

The flow field boundary conditions are as follows: the pressure at the inlet of gap is $P_0 = P_u + P_\gamma + P_e$, the dynamic pressure is $P_u = \frac{\rho u_0^2}{2}$, the viscous friction drag is $P_\gamma = \lambda \frac{L}{D_h} P_u$, and $P_e$ is the pressure at the outlet of balance gap.

The mathematical model of flow field in processing gap could be obtained as follows:

$$\begin{cases} \rho u \cdot \nabla u = \nabla\left[-pI + \eta\left(\nabla u + (\nabla u)^T\right)\right] \\ P_0 = P_u + P_\gamma + P_e \\ P = P_e \end{cases} \tag{4}$$

### 2.3 Simulation and analysis of flow field

Accordingly, the boundary conditions set the pressure at the inlet and outlet of gap, taking the zone of electrolyte flow field in the processing gap as the research object and the electrolyte flow direction perpendicular to the inlet section; the pressure at the inlet of gap is $P_0$, the pressure at the outlet of gap is $P_e$, and the boundary is non slip wall. The electrolyte flow field meshing in processing gap is shown in Fig. 6.

The 3D model of electrolyte flow field simulation result is shown in Fig. 7. The simulation result shows that the distribution of electrolyte flow field is not uniform, the electrolyte at the inlet of the gap is full, but at the end of the machining gap is not full. According to the simulation result, the cathode is extremely easy to short-circuit and burn due to electrolyte insufficiency in the actual processing, which is unable to continue.

The cutaway view of simulation results of electrolyte flow field in machining gap is shown in Fig. 8a; the distribution of the flow field in the machining gap is intuitively shown in the picture. From the simulation result, we can see that the color of the flow field in machining gap gradually turned from red to blue, which means the electrolyte is gradually reduced from the inlet to the outlet along the electrolyte flow direction that is due to the leakage of electrolyte flow. Electrolyte flow in the gap is not sufficient, and cathode is easily burned by electric short circuit. This situation will directly affect the machining

**Table 1** Chemical composition of test piece (weight percent)

| Element | Fe | C | Si | Mn | Cr | Mo | Ni | P | S |
|---|---|---|---|---|---|---|---|---|---|
| Percentages | Balance | 0.42 | 0.27 | 0.60 | 1.10 | 0.20 | 0.03 | 0.03 | 0.03 |

**Table 2** The process parameters

| The process parameters of ECM experiments | | | |
|---|---|---|---|
| Voltage, V | 18 | 17 | 16 |
| Feed rate, mm/min | 4.0 | 5.0 | 6.0 |
| Electrolyte composition | NaCl | | |
| Concentration, g/l | 15% | | |
| Electrolyte temperature, °C | 35 | | |
| Electrolyte pressure, MPa | 2.0 | | |

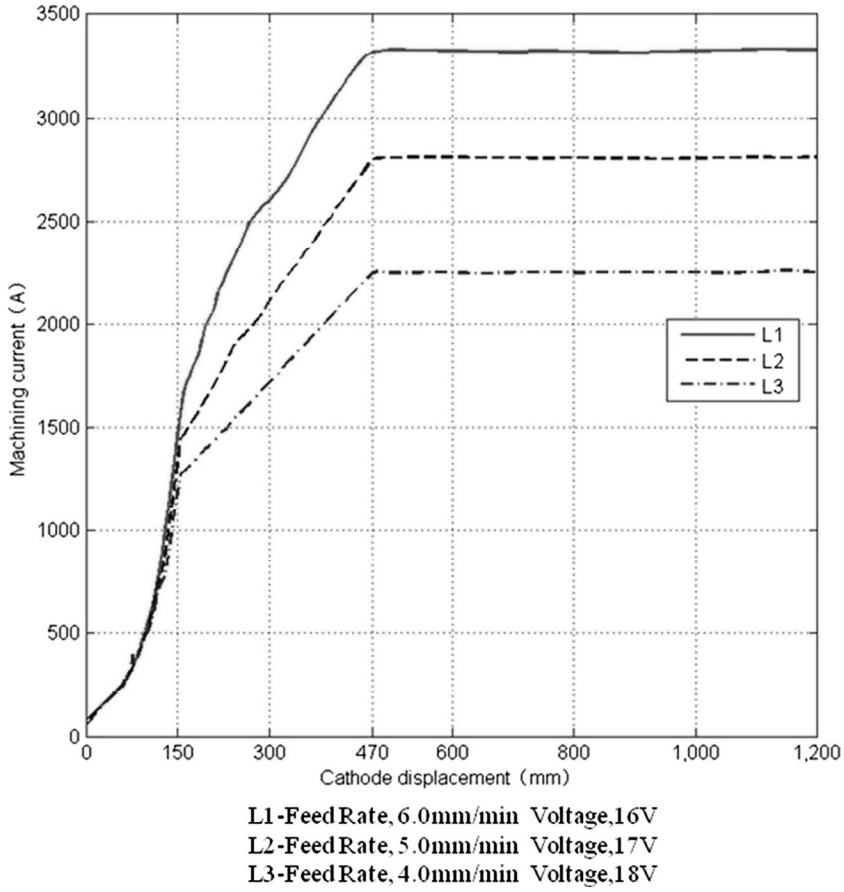


**Fig. 11** Electric current curve

accuracy and machining stability. In order to improve the insufficient electrolyte flow, we setup the added liquid hole on the cathode for supplying the electrolyte flow leakage in the gap, to guarantee the electrolyte at the end of machining gap. The result of simulation is shown in Fig. 8b; from it, we can see that the color distribution of flow field in the gap is significantly improved, and it also shows that the distribution of electrolyte flow is fully supplied.

According to the simulation result, the cathode structure is optimized; the added liquid hole is set up on the cathode working zone to increase the electrolyte flow at the end of the gap, and improve the distribution of electrolyte flow field

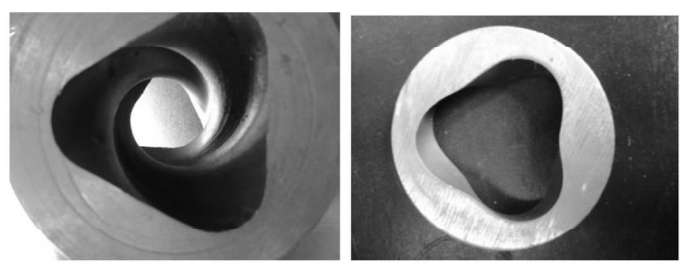

(a) The test piece cross section profile picture

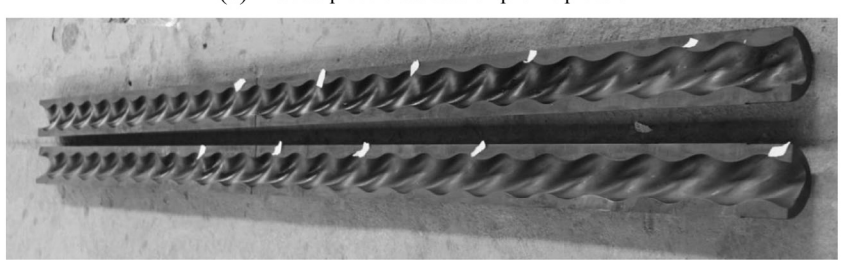

(b) The test piece along the axial section picture

**Fig. 12** ECM process test piece anatomy pictures. **a** The test piece cross-section profile picture and **b** the test piece along the axial section picture

**Fig. 13** The detection equipment

in the relevant machining gap zone. This method can effectively relieve the problem of cathode short-circuit burn. The optimized cathode structure is shown in Fig. 9.

## 3 Process experiments

The experiment was carried out in the DJW-08 CNC horizontal ECM machine as shown in Fig. 10. The test piece size is φ110 × 4000 mm, inner hole is φ37 mm, and the chemical composition is shown in Table 1. The test piece is clamped in the fixture, and the electric conduction device is fixed in the middle of the test piece; the pull rod pass through the test piece inner hole and connected with the cathode. In the machining process, the drive box of the machine drag the pull rod, that drive the cathode, which realized the motion in the test piece inner hole based on the lead of screw pump stator.

### 3.1 The process parameters of ECM experiments

According to the process parameters of ECM experiments in Table 2, the experiments were divided into three groups; the electric current changes with the cathode displacement of each group experiment as shown in Fig. 11.

Figure 11 shows the role of electric current changes with the cathode displacement in the process experiments are basically same. In the cathode displacement range from 0 to 150 mm, the cathode working zone enters the test piece gradually and the current increases with the increase of the processing area. In the cathode displacement range from 150 to 470 mm, the cathode working zone is completely into the test piece and the current gradually increased to stable processing current. In the cathode displacement range from 470 to 1200 mm, the cathode is into the stable process zone, the machining gap becomes balanced, and processing current tends to stable.

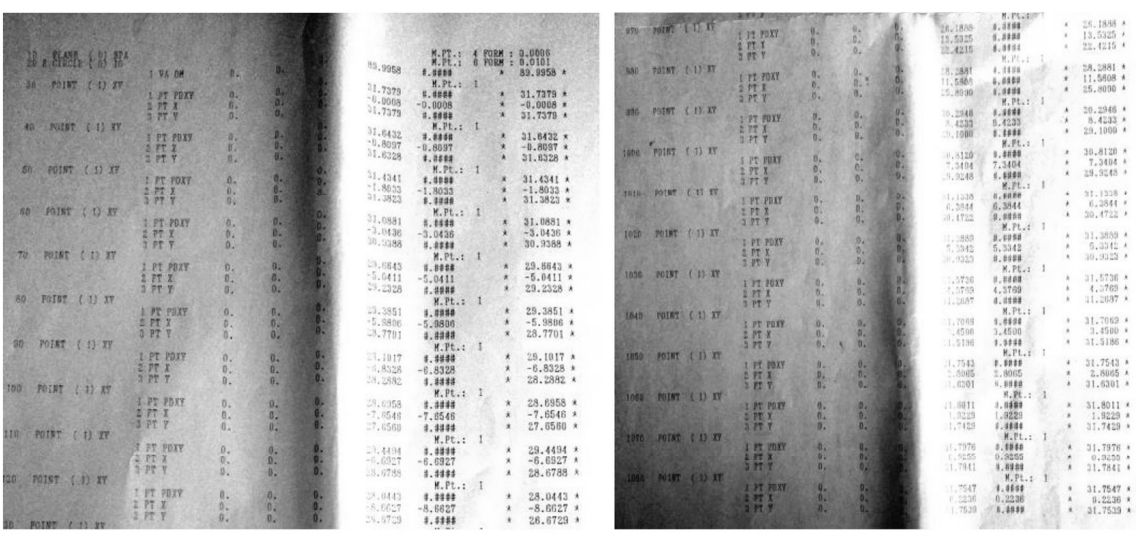

**Fig. 14** Parts of the detection data

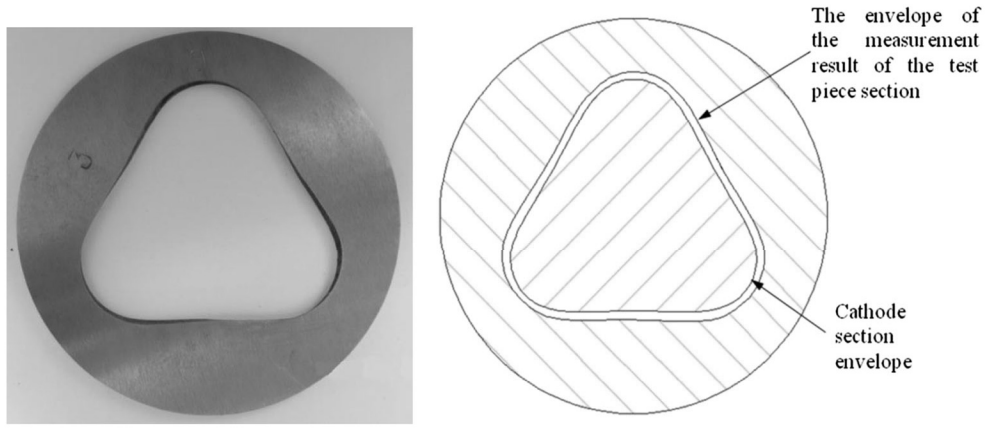


(a) The test piece section (b) The measurement result

**Fig. 15** Experiments result when processing voltage was 16 V, feed rate was 6 mm/min, and electric current was 3320 A. **a** The test piece section and **b** the measurement result

### 3.2 The process experiments result

According to the different process parameters of ECM experiments, the test pieces after the experiment measure the shape and size of test pieces cross-section in different parameters. Based on the measurement results of the test pieces, cross-section in different parameters, compared with the section of the test pieces shape and the cross section of cathode shape, optimized the process parameters of ECM (Fig. 12).

### 3.3 The experiments result detection

Taking the coordinate measuring machine as detection equipment, we measure the inner shape of test pieces. As shown in Fig. 13, the type of equipment is GLOBAL STATUS, the measuring range $X$ is 1200 mm, $Y$ is 1500 mm, $Z$ is 1000 mm, and the measurement precision is 0.003 mm.

The output data of the measurement result is polar coordinates, and parts of the detection results are shown in Fig. 14. Each test piece measured for hundreds of data points, and it is difficult to compare all the data points. In order to compare with the theory shape, we put measurement data into graph shape.

### 3.4 Comparison of measurement results and theoretical shape

Draw the shape of the inner hole according to the result of the test piece measurement, compared with the cathode section shape and the shape of the inner hole, as the result of the comparison shown in Fig. 15, the machining gap between the test piece section envelope of measurement result and the cathode section envelope, which is uniform and the accuracy of size is better when processing voltage was 16 V, feed rate was 6 mm/min, and electric current was 3320 A.

Figure 16 shows the result of the comparison between the cathode section shape and the shape of the inner hole; under the process parameters of the experiments, voltage was 18 V, feed rate was 4 mm/min, electric current was 2250 A, the machine gap is lager and the envelope of the test piece measurement distribution is not uniform, the arc section gap is

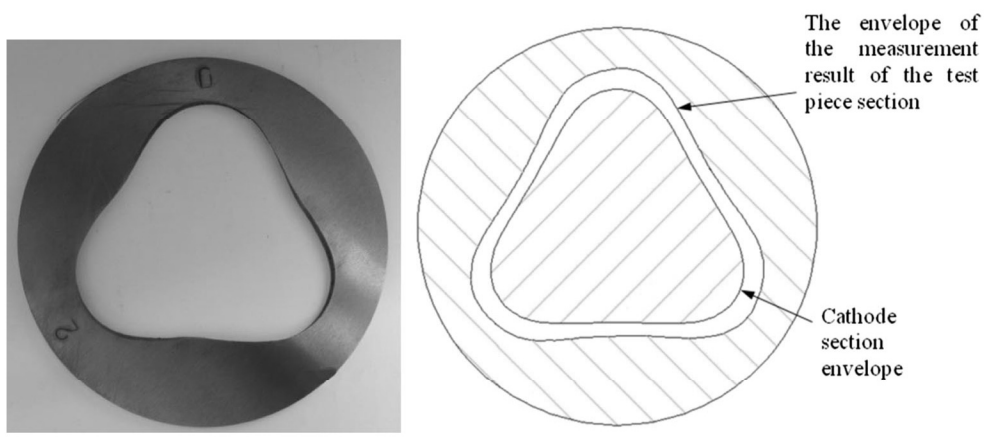


(a) The test piece section (b) The measurement result

**Fig. 16** Experiments result when processing voltage was 18 V, feed rate was 4 mm/min, and electric current was 2250 A. **a** The test piece section and **b** the measurement result

larger than the straight section gap, and the size distribution is not consistent.

The process experiment results show that when the electrolyte temperature is 37 °C, electrolyte pressure is 1.7 MPa, voltage is 16 V, and feed rate is 6 mm/min, the cross-sectional shape size of the test piece processed is consistent with the requirement of the product, and the lead of screw is in accordance with the technical requirements, and the inner spiral hole surface roughness achieves the product drawing requirements.

## 4 Conclusion

COMSOL software was used to simulate the distribution of flow field in ECM machining gap; through analysis, the simulate result can effectively optimize the cathode structure and greatly shorten the design and manufacture cycle of cathode. The COMSOL was used to simulate the distribution of electrolyte flow field in ECM machining gap; the simulation reveals an issue of flow field in the gap, and the electrolyte at the end of the machining gap is not full. In order to solve this problem, an added liquid hole was set up on the cathode working zone to improve the distribution of flow field in the relevant machining gap zone.

In order to obtain the test pieces under different parameters, we carry out experiments which were conducted with different process parameters. The relationship between the parameters and the test pieces inner hole dimension is obtained by measuring the envelope of the test piece. The experiments result show that, when processing voltage was 16 V and feed rate was 6 mm/min, the electrolyte flow field distribution in machining gap is more uniform, effectively improving processing stability, and the dimension reached product requirements. It laid the foundation for the further development of all-metal screw pump stator machining.

**Acknowledgments** The research was supported by the Open Research Fund Program of Shaanxi Key Laboratory of Non-Traditional Machining (grant no. ZSKJ201411).

## References

1. Rajurkar KP, Zhu D, McGeough JA, Kokaz J, De Silva A (1999) New development in electrochemical machining. CIRP Ann Manuf Technol 48(2):567–579
2. Chen ZS, Liu ZL, Yang WY (2012) Experimental research on characteristic of full metal screw pump. Oil Drilling and Production Technology 34:65–67 (in Chinese)
3. Jiang D, Bai N, Li ZL (2014) Numerical simulation and experimental study of the external characteristic of all-metal single-screw pump. China Petroleum Machinery 42(1):77–80 (in Chinese)
4. Paladino EE, Lima JA, Rairam FC (2008) Computational modeling of the three-dimensional flow in a metallic stator progressing cavity pump. Oil and Gas Facilities 9:110–114
5. Adrian C, Aboulghit EM, Alain N (2011) Numerical and experimental studies of simple geometries in slamming. International Journal of Offshore and Polar Engineering 21(3):216–224
6. Li ZL, Shi BN, Lu JQ (2013) Optimum design of all-metal screw pump. China Petroleum Machinery 41(12):97–101 (in Chinese)
7. Ye WD, Han DQ, Song YJ, Du XH (2008) Contacting pressure analysis of stator and rotor of progressive cavity pump. Oil Field Equipment 37(8):25–28 (in Chinese)
8. Fan ZJ, Wang GG, Tang L (2010) Design of device and experiment on magnetic field assisted electrochemical machining. Chinese J Mech Eng 46(1):194–198 (in Chinese)
9. Fan ZJ, Zhao GG, Zhang LJ (2012) Design of anasys-based cathode with complex groove. J China ordnance 8(1):31–34 (in Chinese)
10. Xu ZY, Xu Q, Zhu D, Gong T (2013) A high efficiency electrochemical machining method of blisk channels. CIRPAnn Manuf Technol 62:187–190
11. Westley JA, Atkinson J, Duffield A (2004) Generic aspects of tool design for electrochemical machining. International Symposium on Electrochemical machining 3:77–79
12. Yang F, Fan ZJ, Zhao GG (2010) The research of the ECM machining gap on tube rifings using COMSOL. Machinery Design and Manufacture 4(4):125–127 (in Chinese)
13. Tang L, Gan WM (2014) Utilization of flow field simulation for cathode design in electrochemical machining of aerospace engine blisk channels. Int J Adv Manuf Technol 72:1759–1766
14. Hardisty H, Mileham AR, Shivani HA (1993) Finit element simulation of the electrolechemical machining process. Annals of the CIRP 42(1):201–204
15. Chabert FF, Tancret F (2007) Finite element simulation of interfacial segregation in dilute alloys. J Mater Sci 42:9765–9774